analytical chemistry

Article

pubs.acs.org/ac

193 nm Ultraviolet Photodissociation Mass Spectrometry for the Structural Elucidation of Lipid A Compounds in Complex Mixtures

John P. O'Brien,[†] Brittany D. Needham,[‡] Jeremy C. Henderson,[‡] Emily M. Nowicki,[‡] M. Stephen Trent,[‡] and Jennifer S. Brodbelt*[,†]

[†]Department of Chemistry, The University of Texas at Austin, 1 University Station A5300, Austin, Texas 78712, United States

[‡]The University of Texas at Austin, Department of Molecular Biosciences, 2506 Speedway A5000, Austin, Texas, 78712, United States

Supporting Information

ABSTRACT: Here we implement ultraviolet photodissociation (UVPD) in an online liquid chromatographic tandem mass spectrometry (MS/MS) strategy to support analysis of complex mixtures of lipid A combinatorially modified during development of vaccine adjuvants. UVPD mass spectrometry at 193 nm was utilized to characterize the structures and fragment ion types of lipid A from *Escherichia coli*, *Vibrio cholerae*, and *Pseudomonas aeruginosa* using an Orbitrap mass spectrometer. The fragment ions generated by UVPD were compared to those from collision induced dissociation (CID) and higher energy collision dissociation (HCD) with respect to the precursor charge state. UVPD afforded the widest array of fragment ion types including acyl chain C−O, C−N, and C−C bond cleavages and glycosidic C−O and cross ring cleavages, thus providing the most comprehensive structural analysis of the lipid A. UVPD exhibited virtually no dependence on precursor ion charge state and was best at determining lipid A structure including acyl chain length and composition, giving it an advantage over collision based methods. UVPD was incorporated into an LC−MS/MS methodology for the analysis of a number of structural variants in a complex mixture of combinatorially engineered *Escherichia coli* lipid A.

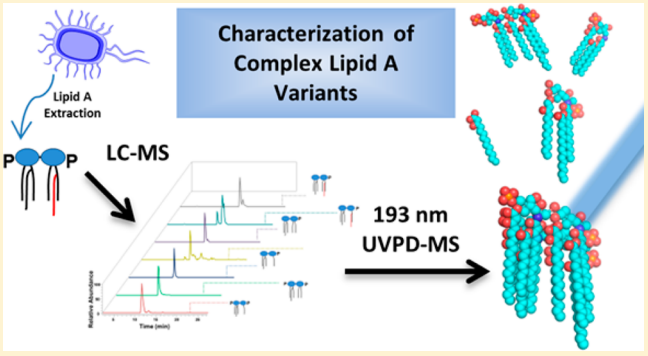

Lipopolysaccharide (LPS) constitutes the outermost layer of the cell membrane in most gram-negative bacteria. LPS is amphiphilic in nature, containing a hydrophilic polysaccharide chain and a hydrophobic membrane anchor known as lipid A. Also called endotoxin, lipid A is typically composed of a bis-phosphorylated diglucosamine with a variable number of amide and ester-linked fatty acid chains. Lipid A is integral to the innate immune response to gram-negative bacteria as it is the moiety of LPS recognized by the mammalian Toll-like receptor 4 (TLR4), which triggers a signaling cascade leading to pro-inflammatory cytokine production.[1] These immunological events initiated by lipid A recognition are important for clearing infection; however, hyperstimulation or overamplification of the immune response can lead to septic shock.[2,3]

Biosynthesis of lipid A proceeds through a well-conserved biochemical pathway. The resultant molecule can be remodeled by various modification enzymes (such as LpxE, LpxF, PagP, PagL, or ArnT) which alter the glycosylation and phosphorylation patterns and number of acyl chains observed in lipid A structure across various gram-negative bacterial species.[3] The fine chemical structure of lipid A is paramount to TLR4 activation and the downstream inflammatory response. Comprehensive investigations of the causal relationship between lipid A structures and affiliated immune response have led to the development of lipid A based vaccines. In particular the production of a vaccine adjuvant using mono-phosphorylated lipid A from *Salmonella minnesota* induces a sufficient immune response without overproduction of inflammatory cytokines.[4] More recently, a combinatorial engineering approach generated 61 *Escherichia coli* strains producing unique lipid A profiles that varied in phosphorylation and acyl chain patterns.[5] These varied structures induced a broad spectrum of innate immune response and showed promise as new *E. coli*-based vaccine adjuvants. The heterogeneity and structural diversity of lipid A molecules within a bacterial sample poses a significant analytical challenge in chemical characterization of complex lipid A mixtures and impedes their development as vaccine adjuvants.

Mass spectrometry (MS) has emerged as one of the premier tools for elucidation of lipid A structures.[6,7] The amphiphilic nature of lipid A species makes them particularly difficult to separate and ionize. Early analysis of lipid A utilized ^{252}Cf plasma-desorption mass spectrometry (PD-MS)[8−10] and fast atom bombardment mass spectrometry (FAB-MS),[11,12] but

Received: November 22, 2013
Accepted: January 21, 2014
Published: January 21, 2014

   dx.doi.org/10.1021/ac403796n | *Anal. Chem.* 2014, 86, 2138−2145

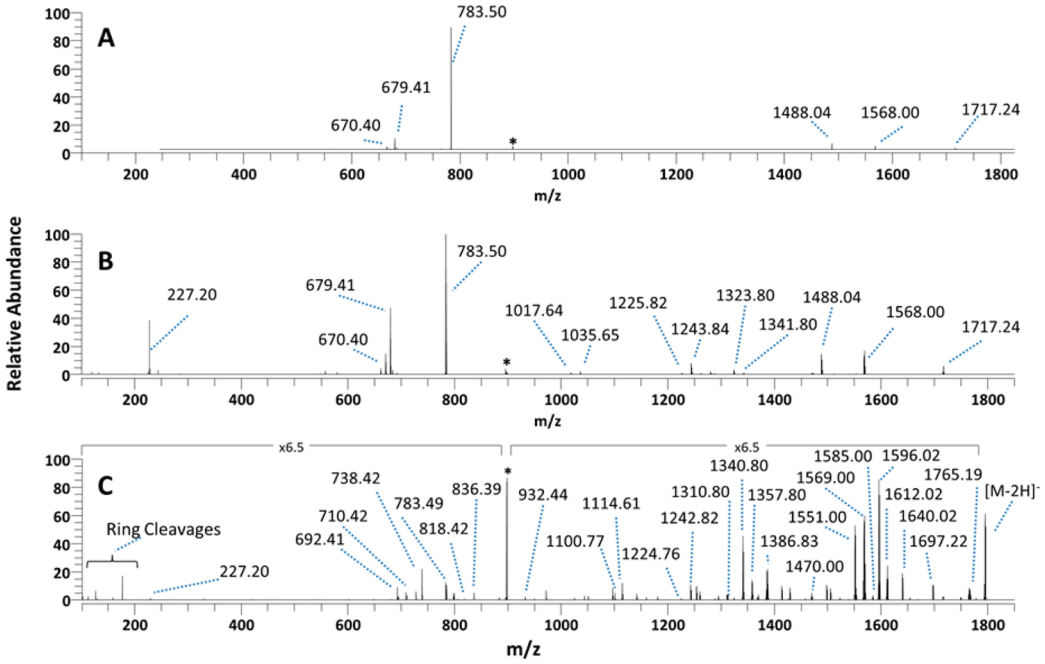

Figure 1. MS/MS mass spectra of doubly deprotonated wild type *E. coli* lipid A (M_r = 1797.2) using (A) CID, (B) HCD, and (C) UVPD. The precursor ion is labeled with an asterisk. Glucosamine fragment ions are labeled as ring cleavages.

both methods have been replaced by matrix assisted laser desperation ionization (MALDI) and electrospray ionization (ESI).[13−31] More recently Yoon et al. demonstrated surface acoustic wave nebulization (SWAN), which was utilized for the ionization of both glycolipids and lipid A and alleviates MALDI matrix effects and emitter clogging during nanoESI.[32] Once ionized, diagnostic fragmentation patterns for structural characterization and differentiation of lipid A molecules are often difficult to interpret. Collision induced dissociation (CID) has proven to be the benchmark tandem mass spectrometry (MS/MS) technique for elucidation of several gram-negative lipid A.[13−32] However, CID tends to selectively cleave the most labile bonds, which frequently results in an insufficient number of fragment ions and prevents fragmentation at important lipid A modification sites. This shortcoming is more commonly observed for multiply deprotonated lipid A species,[18] which is especially problematic in the negative mode for those lipid A molecules decorated with acidic modifications on the glucosamine sugars. Since low energy CID does not always provide sufficient fragmentation, other MS/MS strategies have been explored[19,20,33] as well as MS^n methods which provide both genealogical insight about consecutive fragmentation pathways as well as hierarchical information useful for deeper characterization of lipid A structures and modifications.[17−31] The use of MS^n methods are less amenable to high throughput liquid chromatography (LC)−MS applications and require more elaborate processing for data interpretation. We have recently explored the use of photodissociation methods, including infrared multiphoton dissociation (IRMPD) and ultraviolet photodissociation (UVPD), for the characterization of lipid A.[33−37] UVPD led to the production of an impressive array of diagnostic fragment ions that facilitated mapping of unique modifications.[33−37] UVPD has gained widespread acceptance as a frontier higher energy MS/MS technique that rivals or in some cases outperforms conventional CID methods for both broad profiling of biopolymers and more selective chromophore-mediated approaches.[33−35,38−57] UVPD has been applied to a wide range of bioanalytes including nucleic acids,[40−43] peptides and proteins,[44−52] glycans and oligosaccharides,[53,54] and more recently lipids[55−58] and lipid A molecules.[33−37]

In this study, we present a systematic MS/MS comparison of singly and doubly charged lipid A using CID, HCD, and UVPD on an Orbitrap mass spectrometer for analysis of strains of lipid A from wild types *E. coli*, *Vibrio cholerae*, and *Pseudomonas aeruginosa*. We demonstrate that UVPD, unlike CID and HCD, does not exhibit a significant charge state dependence on the formation of informative fragment ions. We also report a high-throughput LC−UVPD-MS/MS method to separate and analyze low abundance but biologically relevant lipid A variants from engineered *E. coli* strain BN2 expressing key phosphatase, deacylase, and acyltransferase enzymes LpxE, PagL, and PagP, respectively, to aid in the development of new lipid A-based adjuvants in vaccines.

EXPERIMENTAL SECTION

Reagents and Solutions. Bacterial cultures of *E. coli* (hexa-acyl (wild type) BN1 and penta-acyl BN2),[5] and *V. cholerae* (E7946 O1 biotype El-Tor)[36] were grown in 1 L of Luria broth (LB) to an OD_{600} of 1.0. *P. aeruginosa* (PA14) was grown in synthetic cystic fibrosis medium (SCFM).[59] Lipid A was isolated by the Bligh−Dyer method as described previously.[5,34] Residual sodium dodecyl sulfate (SDS) from the purification was removed by washing lipid A with acidified ethanol or by diethylaminoethyl (DEAE) cellulose DE52 column purification, as described previously.[36,37] Solvents for HPLC−MS and direct infusion were purchased from Sigma Aldrich, (St. Louis, MO).

Mass Spectrometry and Liquid Chromatography. All experiments were performed in the negative mode using a Thermo Fisher Orbitrap Elite mass spectrometer (Bremen, Germany) modified to perform ultraviolet photodissociation (UVPD) within the higher collision energy dissociation (HCD) cell in the negative mode using a recently described setup.[49,58] The mass spectrometer was equipped with a Coherent ExiStar

dx.doi.org/10.1021/ac403796n | *Anal. Chem.* 2014, 86, 2138−2145

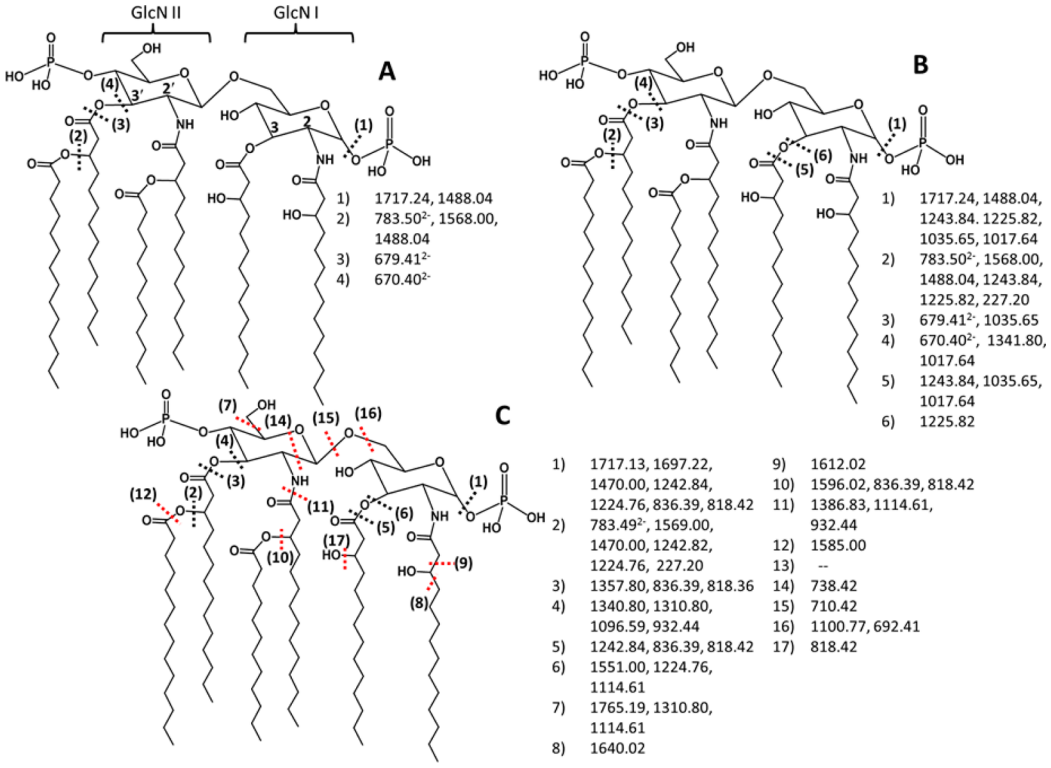

Figure 2. MS/MS fragmentation maps of doubly deprotonated wild type *E. coli* lipid A (M_r = 1797.2) using (A) CID, (B) HCD, and (C) UVPD-MS. Each cleavage site is numbered, and the fragment ions arising from each cleavage site is listed. Those fragment ions that require multiple cleavages are listed next to each cleavage site. Red cleavages are only seen using UVPD-MS. The positions of the 2, 2′, 3, and 3′ carbons and the GlcN I and GlcNII are labeled in part A.

XS excimer laser (Santa Clara, CA) producing 193 nm photons at a net laser energy of 6 mJ/pulse. The HCD cell was held at 10 mTorr for all experiments. UVPD was performed using 10 laser pulses per scan with a pulse repetition rate of 500 Hz. For HCD, the normalized collision energy was set between 40 and 55% using a 0.1 ms activation time. CID experiments were typically performed with the normalized collision energy set at 35% during a 10 ms activation interval. Solutions of lipid A (1 μM) in 50:50 methanol/chloroform were infused at a flow rate of 3 μL/min. The ESI voltage was set at 4 kV, and the sheath gas flow rate was set at 10 arbitrary units. All MS/MS experiments were performed by isolating precursor ions using a m/z window of 3.

Separation of *E. coli* and other lipid A mixtures were undertaken using a Dionex Ultimate 3000 microbore liquid chromatography system (Sunnyvale, CA) equipped with an XBridge C8 column from Waters (3 mm × 100 mm, 3.5 μm particles). Approximately 1 μg of sample was directly injected onto the column. Mobile phase A consisted of 50:50 methanol/water with 0.05% ammonium hydroxide and mobile phase B consisted of 40:40:20 isopropyl alcohol/chloroform/methanol with 0.05% ammonium hydroxide. Separations were performed using a 25 min linear gradient starting at 15% mobile phase B to 70% mobile phase B before holding at 70% mobile phase B for 5 min and re-equilibrating for 5 min at 15% mobile phase B. ESI survey mass spectra were collected using a m/z range of 700−2000. The five ions of greatest abundance were chosen for subsequent MS/MS activation using the UVPD conditions described above. Cleavage site frequencies were calculated using the following equation:

$$\text{weighted relative frequency} = \frac{\Sigma \text{ abundances of all fragmentations associated with cleavage site X}}{\Sigma \text{ abundances of all fragmentations}} \quad (1)$$

RESULTS AND DISCUSSION

This study reports a comparison of the fragmentation of singly and doubly deprotonated lipid A molecules by CID, HCD, and UVPD. The diverse fragmentation pathways are summarized by using fragmentation maps similar to a manner described previously.[33] Briefly, each cleavage site is labeled with a number, and the fragment ions arising from particular cleavages are shown next to each cleavage number with their associated m/z values. Fragment ions that are consistent with ones evolving from multiple cleavage events are listed next to each of the contributing cleavage sites. For example in Figure 1A (which is discussed in detail later) a fragment ion of m/z 1488.04 arises from cleavage of a phosphate group (cleavage site (1) in Figure 2A) and loss of the 3′ secondary acyl chain (cleavage site (2) in Figure 2A). Depending on the lipid A species analyzed, isobaric fragment ions may also exist. To streamline the presentation of data, only representative cleavage sites are included in the fragmentation maps. The distributions of cleavage sites of ions observed in the MS/MS spectra were analyzed by summing the abundances of all fragment ions associated with a specific cleavage site and dividing by the summed abundance of all fragment ions in a given MS/MS spectrum. This allowed a quantitative and systematic comparison of the dominant cleavage sites for each fragmentation method and each charge state. The resulting cleavage site distributions are presented as histograms.

dx.doi.org/10.1021/ac403796n | *Anal. Chem.* 2014, 86, 2138−2145

MS/MS Activation of Wild Type *E. coli* Lipid A. Wild type *E. coli* lipid A is typically decorated with two phosphorylated groups at the 1 and 4′ positions and four primary hydroxyl-acyl chains at the 2, 3, 2′ and 3′ positions of the glucosamine rings (the 2, 3, 2′, and 3′ numbered positions are shown in Figure 2A). Additionally there are two secondary acyl chains on the 2′ and 3′ hydroxyl-acyl chains, which add to the complexity of the final hexa-acylated lipid A structure. CID, HCD, and UVPD mass spectra of the doubly deprotonated wild type *E. coli* lipid A are shown in Figure 1 (and accurate mass measurements in Table S-1 in the Supporting Information), and their representative fragmentation maps are provided in Figure 2. CID of doubly deprotonated lipid A (Figure 1A) produces one dominant doubly charged fragment ion of m/z 783.50, which corresponds to the loss of one of the secondary 3′ acyl chains (e.g., cleavage site (2) in Figure 2A). Other low abundance fragment ions correspond to C−O cleavage at the 3′ position of the glucosamine ring and loss of the phosphate group. HCD yielded a similar fragmentation pattern to the one observed upon CID (Figure 1B), along with a prominent fragment of m/z 227.20, which is the complementary ion formed upon cleavage of site (2) (shown in Figure 2B). This latter ion was not observed upon CID due to the low mass cutoff. HCD also results in a few other C−O cleavages ((5) and (6)) that are informative for mapping the 3 position acyl chain (Figure 2B). Neither CID nor HCD of doubly deprotonated lipid A produced a sufficiently diverse range of fragment ions to allow confident characterization of the lipid A structure without resorting to more elaborate MS^n modes. UVPD as a high-energy MS/MS technique generated a wider array of fragment ions (Figure 1C), as noted in our earlier studies of singly charged lipids.[33−35] These fragment ions arise from C−O, C−N, and C−C bond cleavages within each of the acyl chains (Figure 2C). These unique bond cleavages afford a richer structural map of lipid A, including characterization of the acyl chain lengths. Additionally UVPD resulted in several informative C−O and cross-ring glycosidic bond cleavages that do not occur upon CID or HCD. These allowed discernment of the acyl chain character of each of the separate glucosamine moieties. In particular, the abundant fragment ion of m/z 738.42 (labeled as cross-ring cleavage site (14) in Figure 2C) confirms the distribution of acyl chains among the two glucosamine rings (i.e., four on the GlcN II ring and two on the GlcN I ring). The UVPD fragment ions were measured with high accuracy in the Orbitrap mass analyzer, thus providing confirmation that the types of cleavages and resulting fragment ion structures shown in Figure 2 are consistent with the measured masses (see Table S-1 in the Supporting Information).

The singly deprotonated wild type lipid A species was also subjected to CID, HCD, and UVPD (see spectra in Figure S-1 in the Supporting Information) and the corresponding fragmentation maps are presented in Figure S-2 in the Supporting Information. CID and HCD (Figures S-1A,B in the Supporting Information) led to similar fragmentation patterns, which included multiple phosphate losses and cleavages at the 3′ and 3 C−O bonds. Additional cleavages at the (10), (13) (15), and (17) sites occurred that were not observed for the doubly charged ion (Figure 1A,B). Several high abundance products in the low m/z mass range observed upon HCD were attributed to fragments from the glucosamine rings. UVPD resulted in a spectrum (Figure S-1C in the Supporting Information) similar to that obtained for the doubly charged lipid A (Figure 1C). UVPD resulted in a wide range of C−C, C−O, C−N acyl chain, and glycosidic cleavages, all of which are useful for the structural characterization of the lipid A species. Unlike CID and HCD, UVPD spectrum did not exhibit a significant dependence on charge state.

The cleavage distributions that lead to meaningful fragment ions for WT *E. coli* lipid A for each activation method are summarized in Figure 3. The preferences for particular

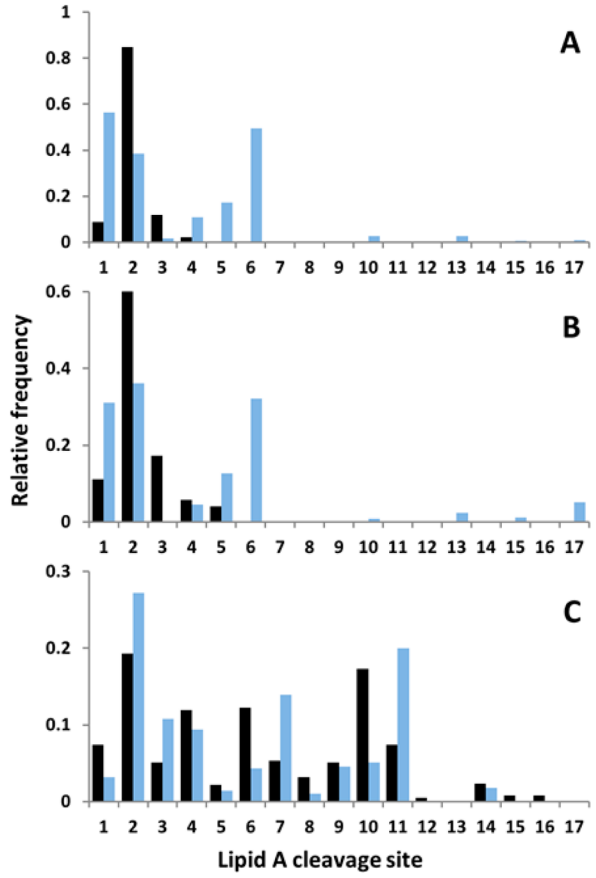

Figure 3. Cleavage site histograms for doubly and singly deprotonated wild type *E. coli* lipid A (1797.2 Da) using (A) CID, (B) HCD, and (C) and UVPD. Black bars represent fragment ions from the doubly deprotonated precursor. Blue bars represent fragments from the singly deprotonated precursor. Relative frequencies for all cleavage sites were calculated using eq 1. The numbers representing the cleavage sites are shown in Figure 2

fragmentation processes were compared by constructing histograms of the relative frequencies of each cleavage site weighted by the abundances of the ions arising from those cleavage sites. The distributions were calculated using eq 1. On the basis of the histograms, it is evident that far fewer cleavage types occur for doubly deprotonated lipid A compared to singly deprotonated lipid A for CID and HCD. In contrast, UVPD results in a much more diverse array of fragment ions, with broad distributions of cleavage sites for both singly and doubly charged ions. For UVPD, the most dominant cleavage sites included (2), (3), (4), (6), (10), and (11), which consisted of a mixture of C−O and C−N cleavages. Elucidating the exact location and lengths of lipid A acyl chains along with the number of phosphorylation sites is imperative as these functionalities modulate the TLR4 immune response. For instance it was shown previously that hexa-acylated *E. coli* lipid

dx.doi.org/10.1021/ac403796n | *Anal. Chem.* 2014, 86, 2138−2145

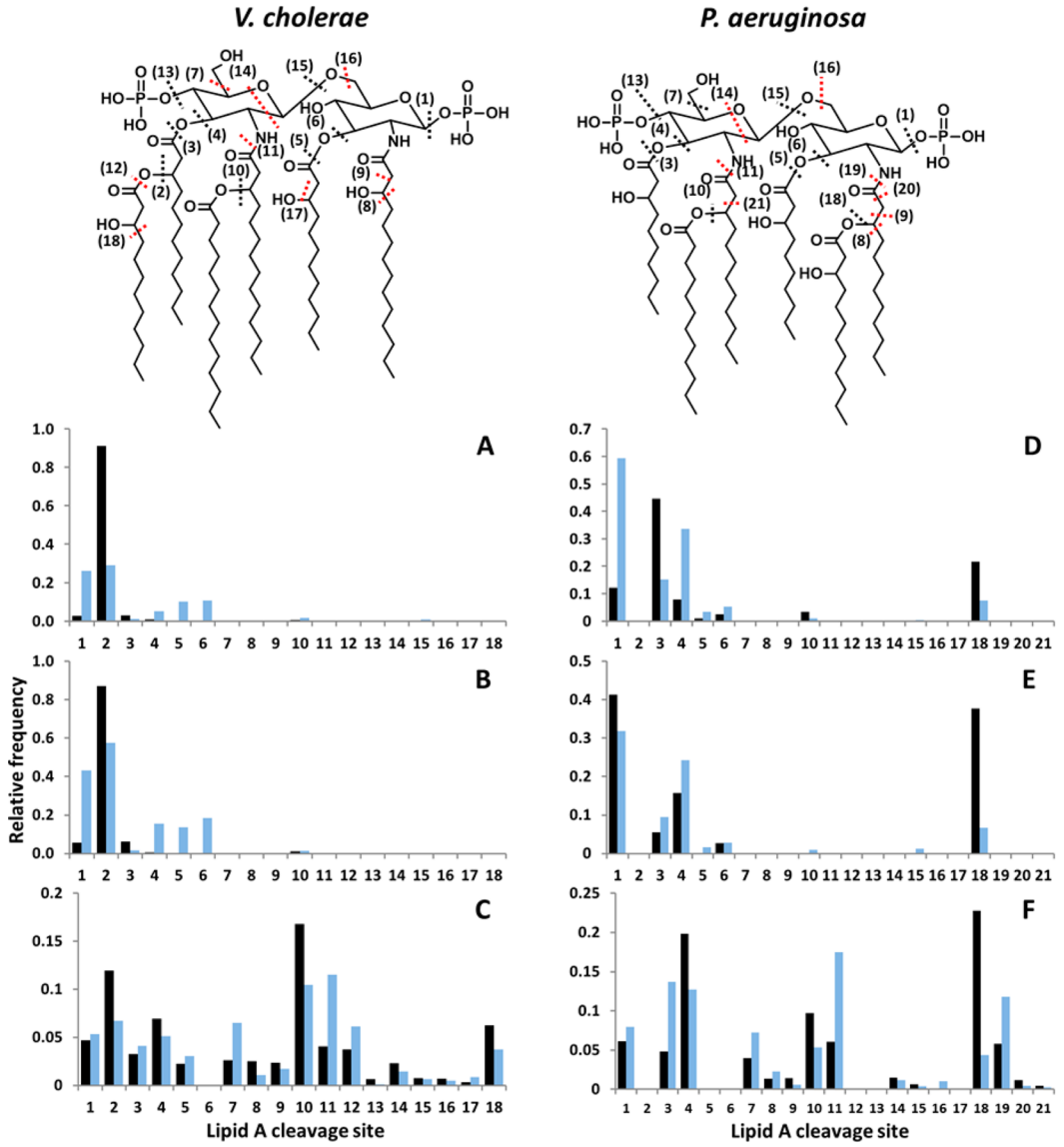

Figure 4. Cleavage site histograms for doubly and singly deprotonated *V. cholerae* lipid A (M_r = 1757.2 Da) (A, B, and C) and *P. aeruginosa* lipid A (M_r = 1617.00 Da) (D, E, and F) using CID (A and D), HCD (B and E), and UVPD (C and F). Black bars represent fragment ions from the doubly deprotonated precursor. Blue bars represent fragments from the singly deprotonated precursor. Relative frequencies for all cleavage sites were calculated using eq 1. The numbers representing the cleavage sites are shown on the structures. Red cleavages are only seen using UVPD-MS.

A species exhibit maximum inflammatory activity, whereas hepta-acylated lipid A is 100 times less inflammatory, and tetra-acylated lipid A is antagonistic.[5,60] On the basis of comparison with CID and HCD, UVPD proves more informative in elucidation of lipid A structures.

MS/MS Activation of *V. cholerae* Lipid A and *P. aeruginosa* Lipid A. The structures of *V. cholerae* and *P. aeruginosa* lipid A species (see Figure 4) were characterized by CID, HCD, and UVPD. The structure of lipid A from *V. cholerae* lipid A is similar to that of WT *E. coli* lipid A with the exception of acyl chain composition. As in *E. coli*, the amide linked hydroxyacyl chains at positions 2 and 2′ are 14 carbons in length; however, the ester linked hydroxyacyl chains at positions 3 and 3′ are 12 carbons (hydroxylaurates). The secondary acyl chain attached to the 2′ hydroxyacyl chain is a 14 carbon acyl chain (myristate), two carbons longer than the laurate attached at this position in *E. coli*. Additionally, a 12 carbon hydroxylaurate is attached to the 3′ hydroxyacyl chain, which is two carbons shorter and contains an additional hydroxyl functional group (compared to the acyl chain at this position in *E. coli*.) Annually, *V. cholerae* is responsible for over 300 000 reported cases of the severe diarrheal disease cholera, and the modification of the hydroxyl group on the 3′ secondary hydroxyacyl chain is important for cationic antimicrobial peptide resistance in this organism.[34]

Although the acylation pattern varies depending on the origin of the isolate, wild-type *P. aeruginosa* lipid A is commonly hexa-acylated (see structure in Figure 4). It also contains two phosphate groups located at the 1 and 4′ glucosamine positions, with hydroxylauryl (12 carbons) acyl chains at the 2 and 2′ positions and hydroxycapric (10 carbons) acyl groups adorning the 3 and 3′ positions. *P. aeruginosa* secondary acyl chains also differ from *E. coli* and *V. cholerae* in position and carbon chain length, which is evident with the laurate and hydroxylaurate groups on the respective amide linked 2′ and 2 positions. *P. aeruginosa* is a potentially deadly and highly

dx.doi.org/10.1021/ac403796n | *Anal. Chem.* 2014, 86, 2138−2145

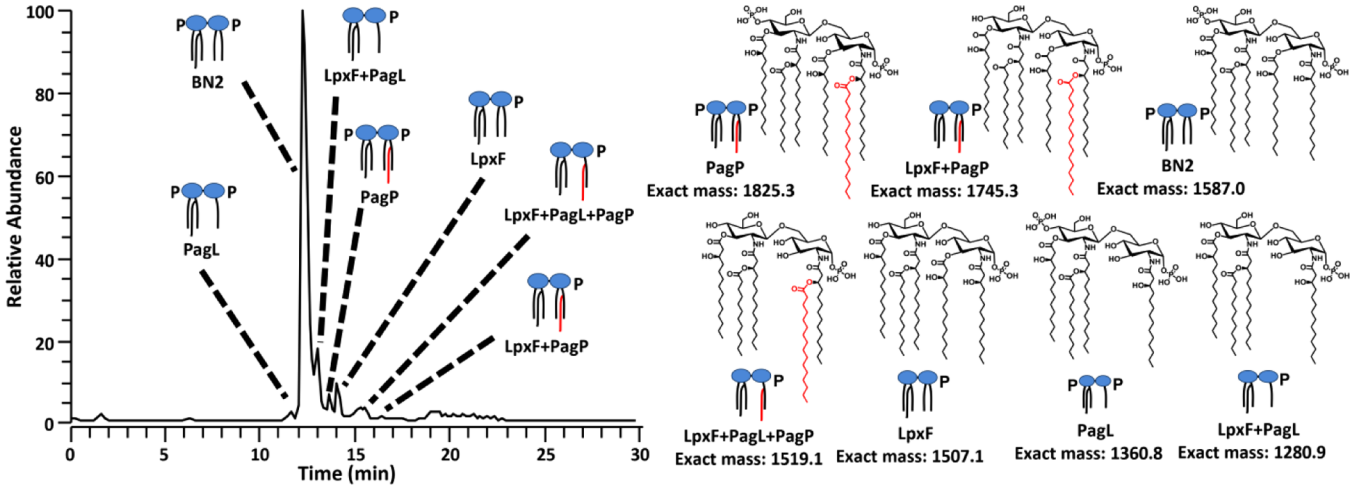

Figure 5. LC−MS trace of a *E. coli* BN2 lipid A strain grown with the enzymes LpxF, PagL, and PagP active. The major lipid A species identified by UVPD are shown with a schematic depiction of each structure and a list of enzymes responsible for the specific modification(s) of each lipid A. The specific PagP enzymatic addition of the palmitate chain is shown in red font. The structures shown on the right are assigned based on the accurate molecular masses of the deprotonated species and the companion UVPD fragmentation patterns.

antibiotic-resistant gram-negative bacterium whose persistence in the human host has been associated with its lipid A acylation pattern.[61]

The CID, HCD, and UVPD mass spectra of the doubly and singly charged precursor species for both *V. cholerae* and *P. aeruginosa* are shown in Figures S3−S6 in the Supporting Information, and the fragmentation maps for each of the spectra are illustrated in Figures S7−S10 in the Supporting Information. The cleavage site histograms for *V. cholerae* and *P. aeruginosa* MS/MS spectra are shown in Figure 4.

The histograms reveal several commonalities for all lipid A molecules independent of fine structural differences. Regardless of charge state, CID and HCD favor preferential cleavage of the phosphate or one of the secondary acyl chains (site (2) for *V. cholerae* or site (18) for *P. aeruginosa* in Figure 4A, B, D, E). There were less dominant contributions representative of C−O bond cleavages at the acyl chains linked on the glucosamine sugars (such as (1), (2), (3), (4), (5), and (6)). The CID and HCD behavior of *P. aeruginosa* lipid A also displayed an increase in fragmentation generated from cleavage of the first primary acyl chain attached to the 3′ position (cleavages (3) and (4)). These product ions were not as notable for lipid A molecules that contained a secondary acyl chain attached to the 3′ primary hydroxyacyl chain. Although the CID (Figures 3A and 4A,D) and HCD (Figures 3B and 4B,E) fragmentation trends are self-consistent, the limited number of cleavage sites limits the ability to fully characterize the lipid A structures.

UVPD generated the most diverse array of fragment ion types arising from a greater number of observed cleavage sites for *V. cholerae* and *P. aeruginosa* (parts C and F of Figure 4, respectively). UVPD of *V. cholerae* resulted in a unique C−C cleavage (cleavage site (18)), producing the diagnostic fragment ion of m/z 1627.99 that allows elucidation of the key hydroxyl group on the 3′ acyl chain. The presence of this modification affects membrane fluidity and influences antimicrobial peptide resistance.[34] The ability to identify important yet subtle modifications of lipid A is imperative for correlating immune responses with lipid A structures. UVPD promoted a mixture of C−O cleavages of both primary and secondary acyl chains and many unique C−N amide cleavages (Figure 4C,F). The (11) and (19) C−N cleavages upon UVPD facilitated the identification of the 2 and 2′ chains, and the (9), (10), (18), (20), and (21) cleavages helped unravel the nature of the constituent secondary chains. One interesting feature is the apparent preferential cleavage of C−N over C−O bonds for amide-linked acyl chains containing secondary amines for singly deprotonated lipid A. This is evident by observing the preference for the C−N bond cleavage (11) over the C−O cleavage site (10) in Figures 3C and Figure 4C,F. A similar trend occurs for the (18)/(19) cleavages associated with the 2 acyl chain in Figure 4F.

Analysis of Lipid A Variants from Engineered *E. coli* Strains. The results described above were acquired via direct infusion and ESI-MS/MS of individual, isolated lipid A compounds. The excellent performance of UVPD for structural characterization and the lack of need for more elaborate MS^n strategies motivated the adaptation of UVPD for an LC−MS workflow for analysis of more complex mixtures of lipid A. Chromatographic separation of lipid A compounds is particularly challenging due to the hydrophobicity arising from the nonpolar acyl chains which renders the compounds most soluble in methanol/chloroform solvents. Extensive optimization led to the use of a reversed phase approach with a C8 microbore column and a mixed organic/aqueous mobile phase, which provided a balance between adequate separation, solubility, and ESI efficiency. The best mobile phase combination was a binary gradient consisting of 50:50 methanol/water with 0.05% NH_4OH and a 40:40:20 mixture of isopropyl alcohol/chloroform/methanol with 0.05% NH_4OH. This LC method in combination with UVPD-MS was used for the analysis of a mixture of lipid A species produced in *E. coli* upon combinatorial modification of the penta-acylated BN2 strain of lipid A. The BN2 strain of lipid A was re-engineered to express specific enzymes that modulate the synthesis of lipid A. For example, the BN2 pFLP strain incorporated the 4′ phosphatase LpxF, the 3 acyl chain deacylase PagL, and the 2 acyl chain palmitoyltransferase PagP.[5] Using a combinatorial approach a vast array of lipid A variants were produced, to promote differential TLR4 stimulation and cytokine responses, in order to develop new adjuvants in vaccines. The production of a number of lipid A variants is possible from the combinatorial gene manipulation

dx.doi.org/10.1021/ac403796n | *Anal. Chem.* 2014, 86, 2138−2145

process, and this provides impetus for the development and application of an LC−UVPD-MS approach to analyze the resultant complex mixtures of lipid A molecules.

The LC−MS trace obtained for the lipid A species originating from the *E. coli* BN2 strain is shown in Figure 5 with the schematic depiction of the identified lipid A structures. Seven lipid A species were identified based on the UVPD mass spectra, ones that contained four to six acyl chains of varying lengths. The lipid A products are categorized based on those enzymes that were responsible for their modification and are annotated in Figure 5, as listed in the order of elution: PagL, unmodified BN2, LpxF + PagL, PagP, LpxF, LpxF, LpxF + PagL + PagP, and finally LpxF + PagP. This elution order paralleled the increases in hydrophobicity of each lipid A species based on the total number and lengths of attached acyl chains and decreases in polarity based on the number of phosphate groups attached to the glucosamine groups. Several other lower abundance lipid A species were also identified with variable acyl chain lengths and other degrees of saturations compared to the seven major species identified which was apparent via the mass shifts of 28.03 (i.e., C_2H_4 unit) or 2.02 Da (H_2) for the molecular species (data not shown). Satisfactory separation of the lipid A mutants was achieved based on the extracted ion chromatograms of each lipid A species as shown in Figure S-11 in the Supporting Information. Adequate chromatographic resolution is obtained even for ones with subtle structural variations such as PagP and LpxF + PagL + PagP, which differ by one phosphate group. The companion UVPD mass spectra allow confident structural assignments, especially given the high accuracy measurements of the molecular ions and fragment ions (mass errors less than 5 ppm) (Figure S-12 in the Supporting Information).

Each lipid A species was subjected to CID and UVPD for structural characterization. Examples of the CID and UVPD mass spectra, the companion fragmentation maps for all lipid A identified in Figure 5 are shown in the Supporting Information (all inclusive in Figures S-13 and S-14). The accurate mass measurement information for single deprotonated BN2 lipid A is provided in Table S-2 in the Supporting Information. The cleavage site histograms for BN2 lipid A (Figure S-13 in the Supporting Information) are analogous to the ones presented earlier, with the histogram for CID dominated by phosphate loss and acyl chain cleavage, while the histogram for UVPD shows a much greater array of diagnostic ions, including those arising from C−O, C−C, C−N, and glycoside and cross-ring cleavages that are not observed upon CID. UVPD provided a richer array of fragment ions (C−C, C−N, and C−O bond cleavages), which facilitated differentiation of the lipid A species in the mixture. In particular, lipid A species modified by the PagP enzyme (the modification is shown in red font in Figure 5) all display the loss of 256 Da, indicative of the presence of an additional palmitate chain attached to the hydroxyacyl chain at position 2. The UVPD spectra of lipid A modified by the phosphatase LpxF (Figure S-14 in the Supporting Information) do not exhibit any phosphate neutral losses, which differed from those lipid A species containing both 1 and 4′ phosphate groups (Figure 5). Those lipid A molecules modified by PagL (Figure 5) were identified by UVPD-specific cross ring cleavages. In particular the fragment ion of m/z 512 is indicative of a lipid A species with only a single acyl chain on the GlcN I glucosamine structure. Identification of all structural mutants of lipid A is critical because different structures modulate the immune response to varying degrees. This is particularly challenging for lipid A mixtures containing low-abundance species like the ones in the BN2 pFLP strain; however LC−UVPD-MS method proved successful for this task.

CONCLUSION

Ultraviolet photodissociation (UVPD) provided the richest array of fragment ions for elucidation of lipid A structures from *E. coli*, *V. cholerae*, and *P. aeruginosa*. HCD and CID resulted in far fewer cleavage sites, and the spectra were dominated by phosphate losses, which limited the ability to characterize lipid A structure by HCD and CID alone. UVPD produced many more unique fragment ions, arising from C−O, C−C, and C−N, glycosidic, and inter-ring bond cleavages. UVPD was combined with a chromatographic method for a high-throughput MS/MS methodology applicable to complex lipid A mixtures. This LC−MS/MS method was successfully applied to the characterization of lipid A species produced by a combinatorially engineered strain of BN2 *E. coli*.

ASSOCIATED CONTENT

Supporting Information

Additional information as noted in text. This material is available free of charge via the Internet at http://pubs.acs.org.

AUTHOR INFORMATION

Corresponding Author

*E-mail: jbrodbelt@cm.utexas.edu.

Notes

The authors declare no competing financial interest.

ACKNOWLEDGMENTS

Funding from the NIH (Grant R01 GM103655 to J.S.B.; Grants AI064184 and AI76322 to M.S.T.), Army Research Office (Grant W911NF-12-1-0390 to M.S.T.), Cystic Fibrosis Foundation (Grant TRENT13G0 to M.S.T.), and the Welch Foundation (Grant F-1155 to J.S.B.) is gratefully acknowledged. We thank Thermo Fisher Scientific with helping on the modifications to the Orbitrap Elite mass spectrometer to allow UVPD.

REFERENCES

(1) Raetz, C. R. H.; Whitfield, C. *Annu. Rev. Biochem.* **2002**, *71*, 635−700.
(2) Trent, M. S.; Stead, C. M.; Tran, A. X.; Hankins, J. V. *J. Endotoxin Res.* **2006**, *12*, 205−223.
(3) Raetz, C. R. H.; Reynolds, C. M.; Trent, M. S.; Bishop, R. E. *Annu. Rev. Biochem.* **2007**, *76*, 295−329.
(4) Casella, C. R.; Mitchell, T. C. *Cell. Mol. Life Sci.* **2008**, *65*, 3231−3240.
(5) Needham, B. D.; Carroll, S. M.; Giles, D. K.; Georgiou, G.; Whiteley, M.; Trent, M. S. *Proc. Natl. Acad. Sci. U.S.A.* **2013**, *110*, 1464−1469.
(6) Kilár, A.; Dörnyei, Á.; Kocsis, B. *Mass Spectrom. Rev.* **2013**, *32*, 90−117.
(7) Banoub, J. H.; Aneed, A. E.; Cohen, A. M.; Joly, N. *Mass Spectrom. Rev.* **2010**, *29*, 606−650.
(8) Caroff, M.; Deprun, C.; Karibian, D. *J. Biol. Chem.* **1993**, *268*, 12321−12324.
(9) Deprun, C.; Karibian, D.; Caroff, M. *Int. J. Mass Spectrom. Ion Processes* **1993**, *126*, 187−190.
(10) Karibian, D.; Brunelle, A.; Aussel, L.; Caroff, M. *Rapid Commun. Mass Spectrom.* **1999**, *13*, 2252−2259.

(11) Seid, R. C., Jr.; Bone, W. M.; Phillips, L. R. *Anal. Biochem.* **1986**, *155*, 168−176.
(12) Johnson, R. S.; Her, G. R.; Grabarek, J.; Hawiger, J.; Reinhold, V. N. *J. Biol. Chem.* **1990**, *265*, 8108−8116.
(13) Cole, R. B.; Harrata, A. K. *Rapid Commun. Mass Spectrom.* **1992**, *6*, 536−539.
(14) Li, J.; Purves, R. W.; Richards, J. C. *Anal. Chem.* **2004**, *76*, 4676−4683.
(15) Casabuono, A. C.; van der Ploeg, C. A.; Rogé, A. D.; Bruno, S. B.; Couto, A. S. *Rapid Commun. Mass Spectrom.* **2012**, *26*, 2011−2020.
(16) Ummarino, S.; Corsaro, M. M.; Lanzetta, R.; Parrilli, M.; Peter-Katalini, J. *Rapid Commun. Mass Spectrom.* **2003**, *17*, 2226−2232.
(17) Cullen, T. W.; O'Brien, J. P.; Hendrixson, D. R.; Giles, D. K.; Hobb, R. I.; Thompson, S. A.; Brodbelt, J. S.; Trent, M. S. *Infect. Immun.* **2013**, *81*, 430−440.
(18) Silipo, A.; De Castro, C.; Lanzetta, R.; Molinaro, A.; Parrilli, M.; Vago, G.; Sturiale, L.; Messina, A.; Garozzo, D. *J. Mass Spectrom.* **2008**, *43*, 478−484.
(19) Jones, J. W.; Shaffer, S. A.; Ernst, R. K.; Goodlett, D. R.; Tureček, F. *Proc. Natl. Acad. Sci. U.S.A.* **2008**, *105*, 12742−12747.
(20) Jones, J. W.; Cohen, I. E.; Turecĕk, F.; Goodlett, D. R.; Ernst, R. K. *J. Am. Soc. Mass Spectrom.* **2010**, *21*, 785−799.
(21) Lukasiewicz, J.; Jachymek, W.; Niedziela, T.; Kenne, L.; Lugowski, C. *J. Lipid Res.* **2010**, *51*, 564−574.
(22) Ting, Y. S.; Shaffer, S. A.; Jones, J. W.; Ng, W. V.; Ernst, R. K.; Goodlett, D. R. *J. Am. Soc. Mass Spectrom.* **2011**, *22*, 856−866.
(23) Schilling, B.; McLendon, M. K.; Phillips, N. J.; Apicella, M. A.; Gibson, B. W. *Anal. Chem.* **2007**, *79*, 1034−1042.
(24) Mikhail, I.; Yildirim, H. H.; Lindahl, E. C. H.; Schweda, E. K. H. *Anal. Biochem.* **2005**, *340*, 303−316.
(25) Shaffer, S. A.; Harvey, M. D.; Goodlett, D. R.; Ernst, R. K. *J. Am. Soc. Mass Spectrom.* **2007**, *18*, 1080−1092.
(26) Kilár, A.; Dörnyei, Á.; Bui, A.; Szabó, Z.; Kocsis, B.; Kilár, F. *J. Mass Spectrom.* **2011**, *46*, 61−70.
(27) El-Aneed, A.; Banoub, J. *Rapid Commun. Mass Spectrom.* **2005**, *19*, 1683−1695.
(28) Madalinski, G.; Fournier, F.; Wind, F.-L.; Afonso, C.; Tabet, J.-C. *Int. J. Mass Spectrom.* **2006**, *249*−*250*, 77−92.
(29) Boué, S. M.; Cole, R. B. *J. Mass Spectrom.* **2000**, *35*, 361−368.
(30) Kussak, A.; Weintraub, A. *Anal. Biochem.* **2002**, *307*, 131−137.
(31) Chan, S.; Reinhold, V. N. *Anal. Biochem.* **1994**, *218*, 63−73.
(32) Yoon, S. H.; Huang, Y.; Edgar, J. S.; Ting, Y. S.; Heron, S. R.; Kao, Y.; Li, Y.; Masselon, C. D.; Ernst, R. K.; Goodlett, D. R. *Anal. Chem.* **2012**, *84*, 6530−6537.
(33) Madsen, J. A.; Cullen, T. W.; Trent, M. S.; Brodbelt, J. S. *Anal. Chem.* **2011**, *83*, 5107−5113.
(34) Hankins, J. V.; Madsen, J. A.; Giles, D. K.; Brodbelt, J. S.; Trent, M. S. *Proc. Natl. Acad. Sci. U.S.A.* **2012**, *109*, 8722−8727.
(35) Hankins, J. V.; Madsen, J. A.; Needham, B. D.; Brodbelt, J. S.; Trent, M. S. In *Bacterial Cell Surfaces*; Delcour, A. H., Ed.; Humana Press: Totowa, NJ, 2013; Vol. *966*, pp 239−258.
(36) Hankins, J. V.; Madsen, J. A.; Giles, D. K.; Childers, B. M.; Klose, K. E.; Brodbelt, J. S.; Trent, M. S. *Mol. Microbiol.* **2011**, *81*, 1313−1329.
(37) Henderson, J. C.; O'Brien, J. P.; Brodbelt, J. S.; Trent, M. S. *J. Vis. Exp.* **2013**, *79*, e50623.
(38) Reilly, J. P. *Mass Spectrom. Rev.* **2009**, *28*, 425−447.
(39) Brodbelt, J. S. *J. Am. Soc. Mass Spectrom.* **2011**, *22*, 197−206.
(40) Smith, S. I.; Brodbelt, J. S. *Anal. Chem.* **2010**, *83*, 303−310.
(41) Smith, S. I.; Brodbelt, J. S. *Anal. Chem.* **2010**, *82*, 7218−7226.
(42) Gabelica, V.; Rosu, F.; Pauw, E.; Antoine, R.; Tabarin, T.; Broyer, M.; Dugourd, P. *J. Am. Soc. Mass Spectrom.* **2007**, *18*, 1990−2000.
(43) Rosu, F.; Gabelica, V.; De Pauw, E.; Antoine, R.; Broyer, M.; Dugourd, P. *J. Phys. Chem.* **2012**, *116*, 5383−5391.
(44) Ly, T.; Julian, R. R. *Angew. Chem., Int. Ed.* **2009**, *48*, 7130−7137.
(45) Yoon, S. H.; Moon, J. H.; Kim, M. S. *J. Mass Spectrom.* **2010**, *45*, 806−814.
(46) Morgan, J. W.; Russell, D. H. *J. Am. Soc. Mass Spectrom.* **2006**, *17*, 721−729.
(47) Guan, Z.; Kelleher, N. L.; O'Connor, P. B.; Aaserud, D. J.; Little, D. P.; McLafferty, F. W. *Int. J. Mass Spectrom. Ion Process.* **1996**, *157*−*158*, 357−364.
(48) Cotham, V. C.; Wine, Y.; Brodbelt, J. S. *Anal. Chem.* **2013**, *85*, 5577−5585.
(49) Shaw, J. B.; Li, W.; Holden, D. D.; Zhang, Y.; Griep-Raming, J.; Fellers, R. T.; Early, B. P.; Thomas, P. M.; Kelleher, N. L.; Brodbelt, J. S. *J. Am. Chem. Soc.* **2013**, *135*, 12646−12651.
(50) O'Brien, J. P.; Pruet, J. M.; Brodbelt, J. S. *Anal. Chem.* **2013**, *85*, 7391−7397.
(51) Enjalbert, Q.; Girod, M.; Simon, R.; Jeudy, J.; Chirot, F.; Salvador, A.; Antoine, R.; Dugourd, P.; Lemoine, J. *Anal. Bioanal. Chem.* **2013**, *405*, 2321−2331.
(52) Diedrich, J. K.; Julian, R. R. *Anal. Chem.* **2010**, *82*, 4006−4014.
(53) Ko, B. J.; Brodbelt, J. S. *Anal. Chem.* **2011**, *83*, 8192−8200.
(54) Racaud, A.; Antoine, R.; Dugourd, P.; Lemoine, J. *J. Am. Soc. Mass Spectrom.* **2010**, *21*, 2077−2084.
(55) Pham, H. T.; Ly, T.; Trevitt, A. J.; Mitchell, T. W.; Blanksby, S. J. *Anal. Chem.* **2012**, *84*, 7525−7532.
(56) Pham, H. T.; Trevitt, A. J.; Mitchell, T. W.; Blanksby, S. J. *Rapid Commun. Mass Spectrom.* **2013**, *27*, 805−815.
(57) Devakumar, A.; O'Dell, D. K.; Walker, J. M.; Reilly, J. P. *J. Am. Soc. Mass Spectrom.* **2008**, *19*, 14−26.
(58) O'Brien, J. P.; Brodbelt, J. S. *Anal. Chem.* **2013**, *85*, 10399−10407.
(59) Palmer, K. L.; Aye, L. M.; Whiteley, M. *J. Bacteriol.* **2007**, *189*, 8079−8087.
(60) Park, B. S.; Song, D. H.; Kim, H. M.; Choi, B.-S.; Lee, H.; Lee, J.-O. *Nature* **2009**, *458*, 1191−1195.
(61) Ernst, R. K.; Hajjar, A. M.; Tsai, J. H.; Moskowitz, S. M.; Wilson, C. B.; Miller, S. I. *J. Endotoxin Res.* **2003**, *9*, 395−400.